DOI: 10.26599/FSHW.2025.9250833

Contents lists available at SciOpen

Food Science and Human Wellness

journal homepage: https://www.sciopen.com/journal/2097-0765

China Food Publishing Co.

Selenium-Enriched Black Soybean Polypeptide Mitigates Benzo(a)pyrene-Induced Hepatotoxicity by Gut-Liver Axis

Ziyan He[#], Yao Meng[#], Lanqi Zhou, Lin Shi[*], Jianke Li[*], Li Yuan[*]

Engineering Research Center of High Value Utilization of Western China Fruit Resources, Key Laboratory of Food Processing Byproducts for Advanced Development and High Value Utilization, College of Food Engineering and Nutritional Science, Shaanxi Normal University, Xi'an 710119, China

ABSTRACT: Selenium (Se)-enriched plant polypeptide represents a premium selenium source possessing numerous physiological functions. Benzo(a)pyrene (BaP) is a carcinogenic food processing contaminant with hepatotoxic properties.The present study aimed to elucidate the mechanism underlying protective effects of selenium-enriched black soybean polypeptide (SeBSPP) against BaP-induced liver injury by integrating liver transcriptome, metabolomics, and gut microbiome. Our study revealed that SeBSPP effectively mitigated BaP-induced liver damage. SeBSPP suppressed the toxicity of BaP on the liver via inhibiting the formation of the carcinogen benzo[a]pyrene-7,8-dihydrodiol-9,10-epoxide-DNA (BPDE-DNA), reducing Aryl hydrocarbon receptor (AhR) enzyme activity and BaP related metabolic enzymes Cytochrome P450 Family (CYP450). Moreover, SeBSPP effectively inhibited liver lipid accumulation and reduced the risk of liver cancer by activating the major urinary proteins (*Mups*), regulating intestinal flora, and increasing the level of short chain fatty acids. Selenium-enriched yeast tablets also exerted a liver protection effect, albeit weaker compared to SeBSPP. This study provides a new direction for preventing hepatotoxicity of BaP and improves Se resource deficiency.

Key words: Selenium enriched black soybean polypeptide, Benzo(a)pyrene, Liver injury, Transcriptomics, Metabolomics, Gut microbiota

1. Introduction

Benzo (a) pyrene (BaP) belongs to polycyclic aromatic hydrocarbons, is a class I carcinogen determined by the World Health Organization[0], and has strong teratogenicity, mutagenicity and accumulation[0]. It widely exists in fried, baked, smoked and other high-temperature processed foods.

Liver is the main target organ of BaP, and BaP exposure can induce a series of liver injury. Cytochrome P450 can biotransform BaP into toxic by-products, resulting in hepatotoxicity[0]. Among them, the generation of 7,8-epoxide from the vacant hydroxyl group on the benzene ring of BaP catalyzed by Cytochrome P450 Family 1 Subfamily A Member 1 (*Cyp1a1*) gene is a classical activation reaction, and 7,8-epoxide is metabolized to produce benzo[a]pyrene-7,8-dihydrodiol-9,10-epoxide (BPDE). BPDE could combine with

[#]Ziyan He and Yao Meng contrubutied equally to this work
***Corresponding author**
Li Yuan: E-mail: yuanli112086@snnu.edu.cn
Jianke Li: E-mail: jiankel@snnu.edu.cn
Lin Shi: E-mail: linshi198808@ snnu.edu.cn

Received 23 June 2025
Received in revised from 8 July 2025
Accepted 25 July 2025

proteins and transcription factors, covalently combine with DNA to cause DNA damage, and then trigger cell carcinogenesis[0]. BaP damages the liver structure and functions, induces oxidative stress and promotes the massive release of inflammatory factors. Such deterious impacts might be attributed to the activation of aromatic hydrocarbon receptors (AhR), disrupting carbohydrate and cholesterol metabolism[00].

Selenium (Se) is an essential trace element for human body. It mainly exists in organisms in the form of Se containing amino acids[0]. It has a variety of physiological functions such as anti-oxidation, immune response, anti-inflammation, anti-cancer and protecting liver[00]. Se rich plant polypeptides are a high-quality Se resource with a variety of physiological functions; Yu et al.[0]observed a protective effect of Se enriched peptides from Cardamine violifolia on high-fat diet induced obesity and its associated metabolic disorders in mice. Previous studies have demonstrated that Se rich black soybean protein (SeBSP) exhibited liver-protective effects. Se enriched black soybean polypeptide (SeBSPP) extracted from SeBSP play crucial roles in organisms, exhibiting various physiological functions due to their low molecular weight and high biological activity[0]. Despite these observed benefits, there is scant research examining the potential of SeBSPP to attenuate BaP-induced liver toxicity, and the underlying mechanisms remain predominantly unexplored.

In the present study, we performed a comprehensive analysis of the potential mitigating effects of SeBSPP on BaP-induced hepatotoxicity, and, for the first time, compared its efficacy with SeBSPP and selenium-enriched yeast tablets (SeYT). Underlying mechanisms of liver protection effects were further explored by integrating liver transcriptome, metabolome and gut microbiome. Our study provides a novel perspective and a strategy for managing BaP toxicity, while also contributing to the enhancement of selenium resources.

2. Materials and methods

2.1 Chemicals and Reagents

BaP was purchased from Sigma (St. Louis, MO, USA). Se-enriched black soybean was provided by Ankang Hanyin Huaye Plant Pharmaceutical Co., Ltd. (Ankang, Shaanxi, China). SeBSPP (< 7kD, Se: 109 mg/kg) were prepared from Se-enriched black soybean by enzymolysis and ultrafiltration. Selenium-enriched yeast tablets (SeYT) were obtained from Mudanjiang Lingtai Pharmaceuticals Co., Ltd (50 μg*50 tablets Se: 714 mg/kg). Assay kits of malonaldehyde (MDA), glutathione peroxidase (GSH-Px), hydrogen peroxide (H_2O_2), total superoxide dismutase (T-SOD), total cholesterol (TC), triglyceride (TG), aspartate aminotransferase (AST) and alanine transaminase (ALT) were obtained from the Nanjing Jiancheng Bioengineering Institute (Nanjing, Jiangsu, China). The bicinchoninic acid (BCA) protein quantification kit was purchased from Thermo Scientific (Rockford, I.L., USA). Aromatic hydrocarbon receptor (AhR) and BPDE-DNA adduct kits were obtained from Shanghai MLBIO Biotechnology Co., Ltd. (Shanghai, China). Total RNA extractor (Trizol) was from Shenggong Biological Engineering Co., Ltd. (Shanghai, China). Transscript all-in-one first-strand cDNA synthesis supermix and PerfectstartTM green qPCR supermix were purchased from Beijing Quanshi Gold Biotechnology Co., Ltd. (Beijing, China). The 4% paraformaldehyde

and olive oil were from Xi'an Jingbo Biotechnology Co., Ltd. (Xi'an, Shaanxi, China). All other chemicals were analytically pure and produced in China.

2.2 Animal and Treatment

Forty-eight male C57BL/6 mice (specific-pathogen-free, 5-week-old) were purchased from the Experimental Animal Center of Xi'an Jiaotong University (Xi'an, China) and kept in standard housing conditions (a 12/12h light/dark cycle,(25 ± 2)℃，60% ± 5% relative humidity) .All mice had free access to autoclaved chow and water. After one week for acclimatization of laboratory environment, the mice were randomly allocated to 6 groups (4 mice/cage and 2 cages/group, n=8) and were orally gavaged for 30 consecutive days. As the protein and BaP were dissolved in distinct solvents, all mice received twice-daily intragastric administrations to negate any potential solvent-related effects. The daily Se intake for mice, set at 25μg/kg, was derived based on the recommended daily Se intake for humans (The Chinese Nutrition Association's 2023 recommendation for daily human Se intake is 50-250 μg/d, with a median value of 150 μg/d). The daily dose of SeBSPP and SeYT were determined to be 229.3 mg/kg and 35 mg/kg per body weight, respectively. The Control group was fed sterile water and olive oil; the BaP group was fed sterile water and BaP (50 mg/kg b.w. , dissolved in the olive oil, corresponding to BaP-inducing genotoxic and carcinogenic effects, as determined in our previous studies[13]); the SeYT group was fed Se yeast tablets (35 mg/kg b.w. , dissolved in normal saline) and olive oil; the SeBSPP group was fed SeBSPP (229.3 mg/kg b.w. , dissolved in normal saline) and olive oil; the SeYT + BaP group was fed Se yeast tablets (35 mg/kg b.w. , dissolved in normal saline) and BaP (50 mg/kg b.w. , dissolved in the olive oil); the SeBSPP + BaP group was fed SeBSPP (229.3 mg/kg b.w. , dissolved in normal saline) and BaP (50 mg/kg b.w. , dissolved in the olive oil). Six hours after the end of the gavage with sterile water, SeBSPP, SeYT, and then BaP and olive oil were administered, respectively. The intervention lasted for 30 consecutive days.

Body weight, food, and water consumption were recorded weekly. Fresh stool samples were collected on the last three days of treatment and immediately stored at -80℃ for further analysis. Following the final administration, mice were fasted for 24 hours. Blood samples were collected from the orbital vascular plexus, followed by cervical dislocation to procure tissue samples. Blood samples were centrifuged at 1200×g for 20 minutes and stored at 4℃. The liver tissue from each mouse was segmented into four sections: one was preserved in 4% paraformaldehyde for histological examination, while the remaining three were flash-frozen in liquid nitrogen and stored at -80℃.

Our animal experimental procedures were approved by the Scientific Ethics Professional Committee of Shaanxi Normal University Academic Committee (Xi'an, Shaanxi, China) and adhered to the guidelines of the Animal Ethical Committee (No. 2024-025).

2.3 Biochemical indicators

The blood samples were centrifuged (4℃, 1200×g, 20 min) to isolate and collect serum samples. The serum levels of TC, TG, AST and ALT were measured by using the reagent kits (Nanjing Jiancheng Bioengineering Institute, Nanjing, China) based on the instructions of manufacturer. The liver tissue samples

were homogenized using an automatic homogenizer (F6/10-10G, FLUKO Equipment Shanghai Co., Ltd., Shanghai, China). After centrifugation (4℃, 5000 r/min, 10 min), the supernatant was collected and determined the total protein concentrations by BCA assay kit. Hepatic concentrations of MDA, T-SOD, GSH-Px and H_2O_2, as well as AhR enzyme activity were measured using commercial kits. For BPDE-DNA adduct assay, liver tissue samples were homogenized with 70% methanol using an automatic homogenizer and filtered with Whatman No 1 filter paper for follow-up experiment. The filtrate was subjected to ELISA according to the instructions.

2.4 Hematoxylin-Eosin Staining

The liver tissues were fixed with 4% paraformaldehyde and then were sent to Wuhan Servicebio Technology Co., Ltd. for HE staining. The slides were observed and photographed under a light microscope.

2.5 RT-qPCR

Total RNA was extracted from liver tissues with Trizol (Shenggong Biological Engineering Co., Ltd., Shanghai, China) according to the manufacturer's instructions, and synthesized corresponding cDNA using Transscript all-in-one first-strand cDNA synthesis supermix. Real-time quantitative polymerase chain reaction (RT-qPCR) was performed using PerfectstartTM green qPCR supermix. The transcription of *Gapdh*, AhR, *Cyp1a1*, *Cyp2a4*, *Mup1*, *Mup11* was detected by SYBR Green system (Table 1). *Gapdh* was used as an internal reference, and PCR reaction procedures were as follows: pre-denaturation at 94 ℃ for 30s, annealing at 94℃ for 5 s, extension at 60℃ for 30 s, 40 cycles in total. After data collection, the relative expression levels of each gene in different treatment groups were analyzed.

Table 1. Primers used for amplification.

Gene	Primer	Length (BP)	Primer information
Gapdh	CCTCGTCCCGTAGACAAAATG (S) TGAGGTCAATGAAGGGGTCGT (A)	133	NM_008084.2
AhR	CTTCATCTTCAGGACCAAACACA (S) GAGTGGCGATGATGTAATCTGGT (A)	296	NM_001314027.1
Cyp1a1	ACCATGACCGGGAACTGTG (S) TGCTGAGGACCAGAAGACCG (A)	307	NM_001136059.2
Cyp2a4	TTCTCAACAGGAAAGCGCATTTG (S) AGATCTGGTACGTTGGAGGTATTT (A)	324	NM_009997
Mup1	TGTGAGAAGCATGGAATCCTTAGA (A) GGGATGCTGTATGGATAGGAAGG (S)	180	NM_031188
Mup11	TGTGAGGAGCATGGAATCATTAGA (A) ACGATGAAAGGCAGATCTCAGAA (S)	179	NM_001164526.1

2.6 Liver transcriptomics

Total RNA was extracted from the liver tissue samples using TRIzol® Reagent based on the manufacturer's instructions. The XX RNA-seq transcriptome librariy was prepared following Illumina® Stranded mRNA Prep, Ligation from Illumina (San Diego, CA) using 1μg of total RNA. Only high-quality RNA samples (OD260/280=1.8~2.2, OD260/230≥2.0, RIN≥6.5, 28S:18S≥1.0, > 1μg) were used for purification, reverse transcription, library construction and sequencing at Shanghai Majorbio Bio-pharm Technology Co.,Ltd (Shanghai, China) according to the manufacturer's instructions (Illumina, San Diego,

CA). Paired-end RNA-seq sequencing library was sequenced via the NovaSeq Xplus sequencer (2 × 150bp read length) on the Illumina NovaSeq 6000 platform. A total of 27923 expression genes and 91701 expression transcripts were detected in this analysis.

2.7 Liver metabolomics

Metabolite extraction was performed on liver tissue samples from each equally divided sample (50mg). The LC-MS/MS analysis was conducted on a SCIEX UPLC-Triple TOF 5600 system at Majorbio Bio-Pharm Technology Co. Ltd. (Shanghai, China). A pooled quality control sample was prepared by mixing equal volumes of all liver tissue samples. Data acquisition was performed with the Information Dependent Acquisition mode and the detection was carried out over a mass range of 50-1000 m/z.The LC/MS raw data were preprocessed by Progenesis QI (Waters Corporation, Milford, USA) software, and a three-dimensional data matrix including sample information, metabolite name and mass spectral response intensity was exported in CSV format. Metabolite annotation was conducted by match m/z and fragmentation against HMDB and Metlin databases as well as in-house library.

2.8 16S rRNA sequencing

Fresh feces of mice were collected for 16S rRNA gene sequencing analysis at Shanghai Majorbio Bio-pharm Technology Co.,Ltd (Shanghai, China). Bacterial genome DNA from fecal samples (n=6) was extracted by a QIAamp DNA Stool Mini Kit (Qiagen, Germany). DNA concentration and purity were measured on 1% agarose gel to control the DNA quality. PCR-amplification of the V3-V4 hypervariable regions of the 16S rRNA genes was then performed using the specific primer with the barcode, and the PCR products were detected and quantified using the QuantiFluorTM -ST Blue fluorescence Quantitative System (Promega). Sequencing libraries were generated using TruSeqTM DNA Sample Prep Kit (Illumina, San Diego, CA, USA), followed by the 16S rDNA high-throughput sequencing using an Illumina MiSeq platform with 250 bp paired-end reads. Subsequently, the paired-end reads were merged using FLASH V1.2.11 and quality-controlled under specific filtering conditions according to QIIME V1.9.1 to obtain high-quality clean tags. In total, 50 families, 116 genera, 180 species were annotated.

2.9 Western-Blot

The total proteins that were isolated from liver tissues with RIPA buffer (Shenggong Biological Engineering Co., Ltd., Shanghai, China.) were resolved with 10% SDS-PAGE and shifted to PVDF membranes. Subsequently, the membranes that were sealed by 5% skim milk were successively introduced to primary antibody against PPARγ or GAPDH overnight at 4 ℃ and HRP-linked secondary antibody. An enhanced chemiluminescence (ECL) detection system was adopted for the visualization of protein bands in accordance with the recommended specifications.

2.10 Molecular docking

To investigate the interaction relationship between lipid metabolites and hub gene, we performed molecular docking studies to explore the binding activity of the two. 3D structure files were downloaded from

RCSB PDB (http://www.rcsb.org/) and 2D structures files were downloaded from PubChem database (http://pubchem.ncbi.nlm. nih.gov/), input the 2D structures into Chem office 20.0 software to make its 3D structure and save as mol2 files. Protein receptors were treated with water molecule and phosphate removal in PyMol2.6.0. Molecular Operating Environment 2019 software was used to minimize the energy of the compounds, pre-treat the target proteins and find the active pocket. Finally, MOE 2019 was run for molecular docking. Evaluated the binding activity of the two based on their binding energy, and the results were visualized by PyMol2.6.0 and Discovery studio2019 software.

2.11 Statistical analysis

All results were conducted by SPSS v19.0 (International Business Machines Corporation, USA). Data are presented as the means ± standard deviation (SD), and were analyzed using the one-way factorial analysis of variance (ANOVA) and Duncan's post hoc test. $P < 0.05$ was considered as a statistically significant. Transcriptomic，metabolomics and 16s analysis were performed using the online platform of Majorbio Cloud Platform (www.majorbio.com).

For transcriptome data，differential expression analysis was performed between groups using the DESeq2, with |log2FC|≥1 and FDR＜0.05 considered to be significantly different expressed genes(DEGs). Functional annotation analysis and functional enrichment analysis were then performed to identify the significant functions and signaling pathways involved in the commonly-regulated genes at Bonferroni-corrected p＜0.05. KEGG pathway analysis was carried out by Python scipy. For metabolomics data, principal component analysis (PCA) and orthogonal least partial squares discriminant analysis (PLS-DA) were performed to evaluate the stability of the model. Venn analysis was carried out on the differential metabolites. For microbiota data, the α-diversity was analyzed on genus and species level to assess the richness and diversity of microbial communities. The β-diversity analyses including principal coordinate analysis (PCoA) was conducted based on weighted_unifrac distance algorithm on OTU level. Cluster analysis of the expression trend of gut microbiota was performed at the family, genus and species levels.

The weighted gene coexpression network analysis (WGCNA, R package WGCNA) was adopted to identify highly synergistic expressed modules containing core genes, metabolites and gut microbes that were predominately modulated by SeBSPP. Model parameters were determined according to previous studies. Correlations between the expression profiles of each module (ME) and Bap related biochemical parameters were calculated. Specific focus was given on the MEs that were highly modulated by Bap and SeBSPP.

3. Results

3.1 SeBSPP alleviates BaP-induced weight reduction and liver dysfunctions

In comparison to the Control group, BaP significantly decreased the growth of body weight (Fig. 1A-D), food intake, and water intake, yet concurrently elevated serum concentrations of TC, TG, AST, and ALT ($P <$ 0.05). Notably, these adverse effects were mitigated by the oral administration of SeBSPP and SeYT, with SeBSPP exhibiting more significant amelioration (Fig. 1E-H).

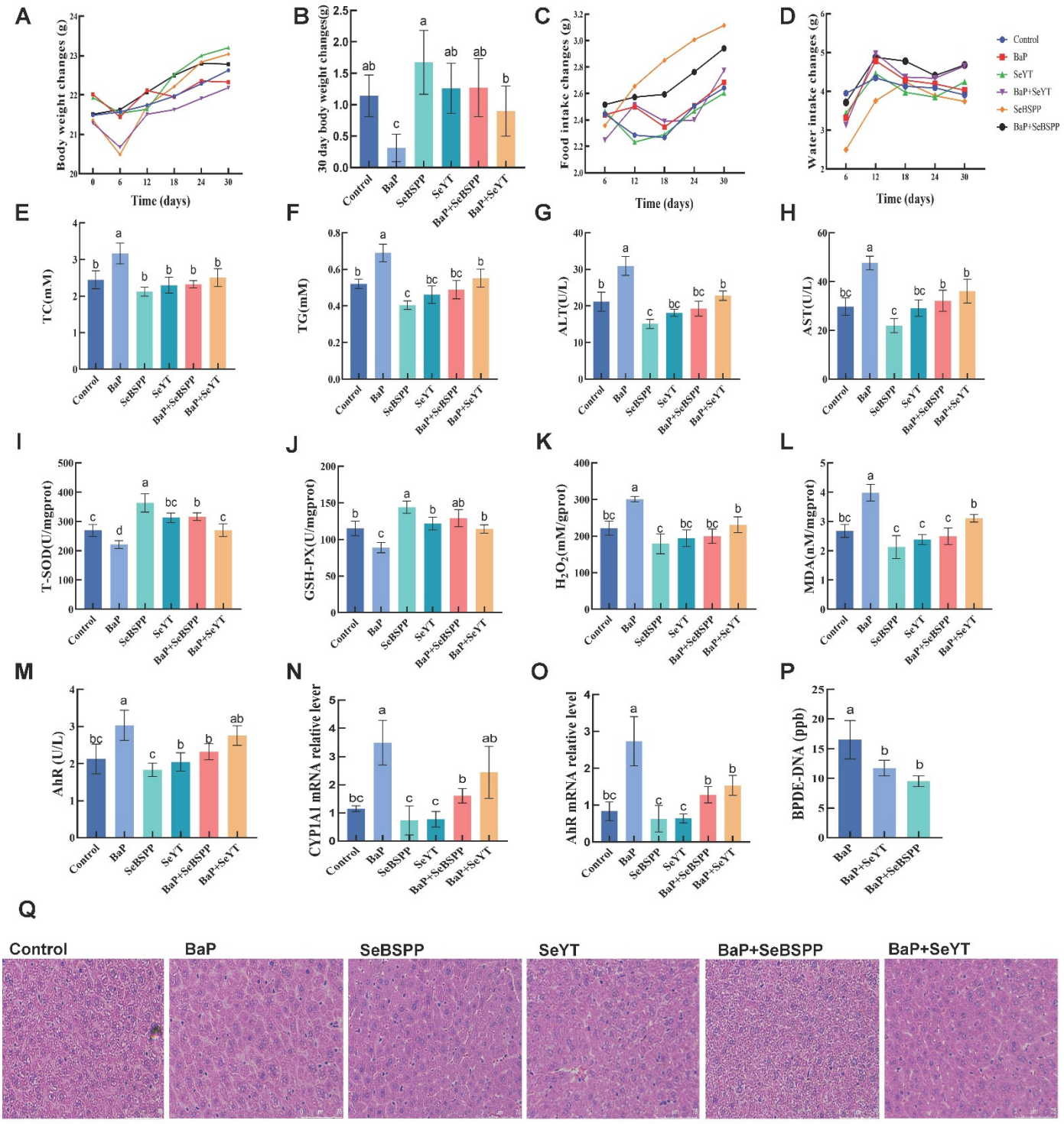

Figure 1. Effects of SeBSPP and SeYT on body weight, food intake, water intake and liver physiological indicators of mice. The body weight, food and water intake of each group were measured every 6 days, and the mean value was calculated to plot. (A) Body weight changes; (B) 30 days body weight gain; (C) Food intake changes; (D) Water intake changes; (E)The level of TC in serum; (F) The level of TG in serum; (G) The level of AST in serum; (H) The level of ALT in serum. And liver samples were homogenized, centrifuged and then processed for the determination of antioxidative function. (I) The activity of SOD; (J) The activity of GSH-Px; (K) The level of MDA; (L) The level of H2O2; (M) AhR enzyme activity; (N) AhR mRNA relative level; (O) Cyp1a1 mRNA relative level; (P) BPDE-DNA content; (Q) H&E staining; Scale bar, 75 μm; These results are shown as the means ± SD, with 6 mice/group, $P < 0.05$. SeBSPP: Selenium-enriched black soybean polypeptide; SeYT: Selenium-enriched yeast tablets; BaP: Benzo(a)pyrene; TC: Total cholesterol; TG: Tri-glyceride; AST: Aspartate aminotransferase; ALT: Alanine transaminase; GSH-Px: Glutathione peroxidase; T-SOD: Total Superoxide dismutase; MDA: Malondialdehyde; H2O2: Hydrogen peroxide; AhR: Aryl hydrocarbon receptor; Cyp1a1: Cytochrome P450, family 1, subfamily a, polypeptide 1.

Oxidative damage leads to abnormal liver function[0]. As shown in Fig. 1Q, histopathological analysis based on H&E staining revealed that the liver cells in the Control group exhibited intact morphology and structur, with round, uniformly sized nuclei and no apparent abnormalities. In contrast, the BaP group showed numerous prominent vacuoles and indistinct nuclear borders, indicating that BaP had caused noticeable liver damage. The vacuolar changes were markedly reduced in the BaP+SeBSPP and BaP+SeYT groups, suggesting that both SeBSPP and SeYT have the potential to alleviate BaP-induced liver injury. Additionally, compared to the control group, the BaP group exhibited significantly lower enzyme activities of SOD and GSH-Px by 17.94% and 22.85%, respectively ($P < 0.05$). The hepatic MDA, a marker of lipid peroxidation, and H_2O_2, a reactive oxygen species, were both significantly elevated in the BaP group by 48.55% and 36.08% (Fig. 1I-L), respectively ($P < 0.05$). Both SeBSPP and SeYT could effectively reverse BaP-induced oxidative damage and the protective effect of SeBSPP was more prominent compared to SeYT. These findings further corroborate the protective role of SeBSPP and SeYT against BaP-induced liver oxidative damage and hepatic steatosis.

Additionally, oral administration of SeYT and SeBSPP had no impacts on TC, AST, H_2O_2 and MDA in mice fed with normal chew. Moreover, SeBSPP reduced TG and ALT while increasing T-SOD and GSH-Px, in relative to the Control.

3.2 Effects of SeBSPP on BaP metabolism-related enzymes and BPDE-DNA adduct

In the livers of mice treated with BaP, AhR enzyme activity was significantly enhanced by 42.65% compared to the control group (Fig. 1M, $P < 0.05$). This enhancement was significantly reduced by SeBSPP ($P < 0.05$). In contrast, no such effect was observed for SeYT. An increase in the mRNA expressions of AhR and CYP1A1 was also observed in BaP group, and notably decreased by SeBSPP (Fig. 1N-O, $P < 0.05$).

Moreover, BaP is metabolized by CYP450 enzymes into the highly carcinogenic BPDE, which subsequently binds to DNA, forming BPDE-DNA adducts and resulting in severe DNA damage (Fig. 1P). As demonstrated in Figure 1P, a significant elevation in BPDE-DNA adduct content was observed in the BaP-exposed group compared to Control group ($P < 0.05$). Exposure to SeBSPP and SeYT significantly reduced the formation of BPDE-DNA by 42.22% and 28.81%, respectively. SeBSPP outperformed SeYT in protecting against BaP-induced genotoxicity compared to SeYT.

3.3 Effects of SeBSPP on liver transcriptome

We investigated the effects of SeBSPP on gene profiles of liver in BaP-exposed mice. BaP upregulated 192 genes while down-regulating 401 genes compared with Control group. SeBSPP in turn enhanced 162 genes while reduced 173 genes relative to the BaP group (Fig. 2A&B). Among the genes studied, 56 exhibited differential expression between BaP and Control, were modulated by SeBSPP (Fig. 2C). Specifically, we observed that BaP suppressed expressions of several *Mups*-related genes, which were restored by SeBSPP. By contrast, SeBSPP reduced BaP-promoted expressions of *Cyp2a4*, *Cyp2b10* and *Cyp2c39* (Fig. 2D). SeYT significantly influenced the hepatic transcriptome, resulting in the upregulation of 106 genes and downregulation of 97 genes compared to BaP (Supple. 1A). Notably, only 25 of these genes exhibited

differential expression between BaP and the Control. Notably, only 7 genes were modified by both SeBSPP and SeYT, including *Acod1*, *Rnf125*, *Pitx3*, *Pask*, *Rgs1*, *Elovl3* and *Gm37988*. Gene expressions that were modulated by SeBSPP were further verified by using RT-qPCR and consistent results were obtained (Fig. 2G-I).

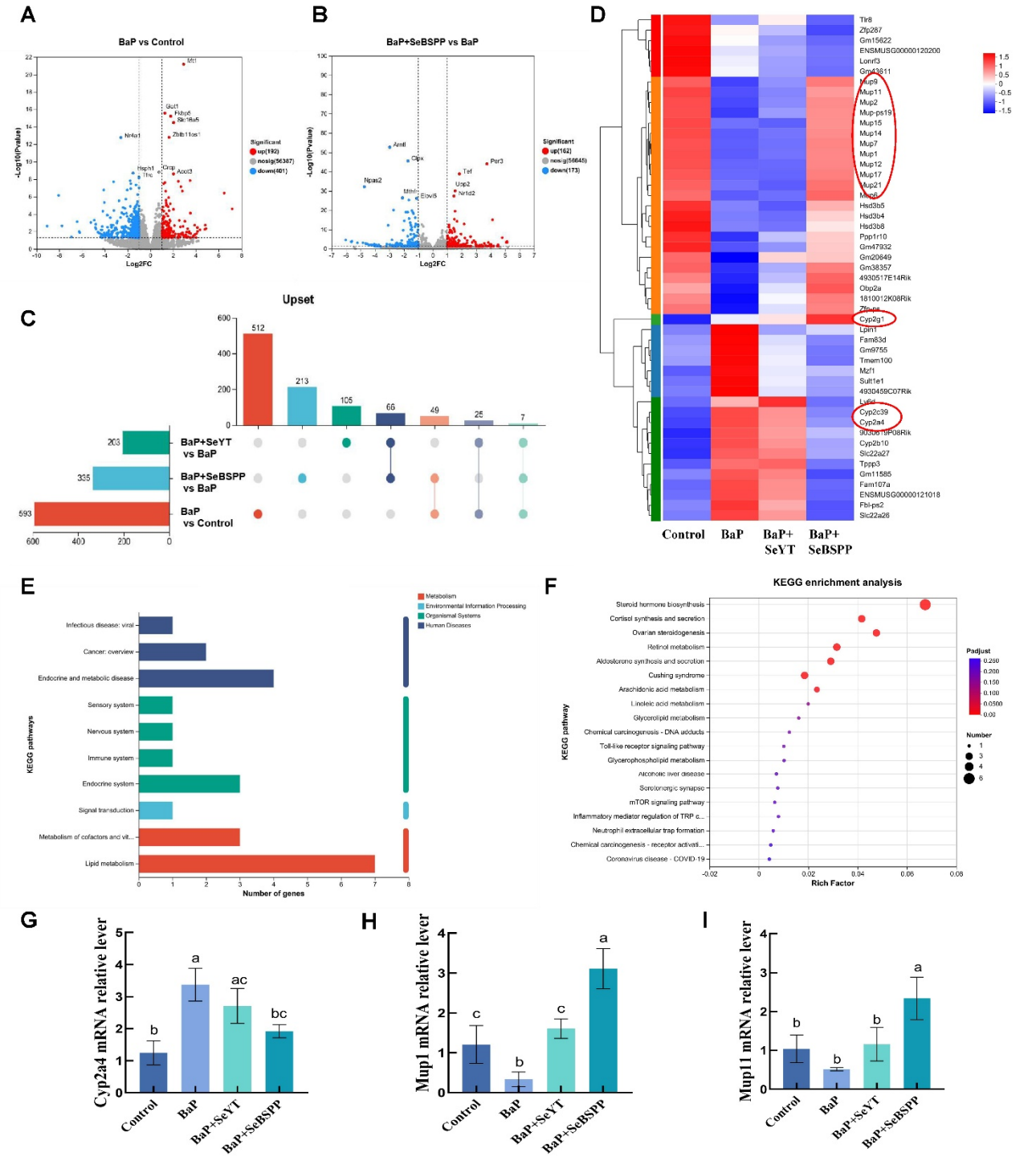

Figure 2. SeBSPP impact on liver transcriptomic.
(A) Volcano plot of differential genes in BaP vs Control; (B) Volcano plot of differential genes in BaP+SeBSPP vs BaP; (C) Upset of differentially expressed genes among four groups; (D) Heatmap of genes both in BaP vs Control and BaP+SeBSPP vs BaP; (E) KEGG pathway classification of BaP vs Control and BaP+SeBSPP vs BaP; (F) KEGG enrichment of BaP vs Control and BaP+SeBSPP vs BaP; (G) Cyp2a4 mRNA relative level; (H) Mup1 mRNA relative level; (I) Mup11 mRNA relative level. These results are shown as the means ± SD, with 6 mice/group, $P < 0.05$. KEGG: Kyoto Encyclopedia of Genes and Genomes; Cyp2a4: Cytochrome P450, family 2, subfamily a, polypeptide 4; Mup1: Major urinary protein 1; Mup11: Major urinary protein 11.

Additionally, SeBSPP-modulated genes were primarily involved in lipid metabolism, endocrine and metabolic disease, metabolism of cofactors and vitamins (Fig. 2E). Among them, 6 genes were enriched in the steroid hormone biosynthesis pathway (Fig. 2F). SeYT affected genes related with cancer and immune system (Supple. 1B). These results collectively indicate that SeBSPP and SeYT could prevent BaP induced liver damage via affecting diverse molecular pathways. SeBSPP exhibited more pronounced effects than SeYT.

3.4 Effects of SeBSPP on liver metabolome

A total of 831 metabolites were identified in the liver, comprising 283 lipids and lipid-like molecules, 215 organic acids and derivatives, 98 organoheterocyclic compounds, 88 organic oxygen compounds, 48 benzenoids, and others (Fig. 3A). Using PLS-DA, a distinct separation was observed between the control group, BaP, SeBSPP, and SeYT. SeBSPP significantly altered the liver metabolome of BaP-exposed mice, resulting in metabolite profiles resembling those of the control group (Fig. 3B).

A total of 184 metabolites were regulated in group of control, BaP, SeBSPP and SeYT. Specifically, BaP upregulated 18 metabolites while down-regulating 22 metabolites compared with control group. SeBSPP in turn enhanced 46 metabolites while reduced 66 metabolites relative to the BaP group (Fig. 3C&D). Among those, 7 metabolites differed between BaP and Control were modulated by SeBSPP (Fig. 3E), including N-Acetyl-D-cysteine, Streptidine, Ecgonine, Cefadroxil, Glutamine-glutamate, Dephospho-CoA and Arborinine. For instance, BaP downregulated the expression of Daidzein, an effect that was reversed by the oral supplementation of SeBSPP. Conversely, SeBSPP mitigated the BaP-induced upregulation of PE(P-16:0/0:0), LysoPC (0:0/16:0), and LysoPE(P-18:1(9Z)/0:0) expressions, as depicted in Fig.3F-I.

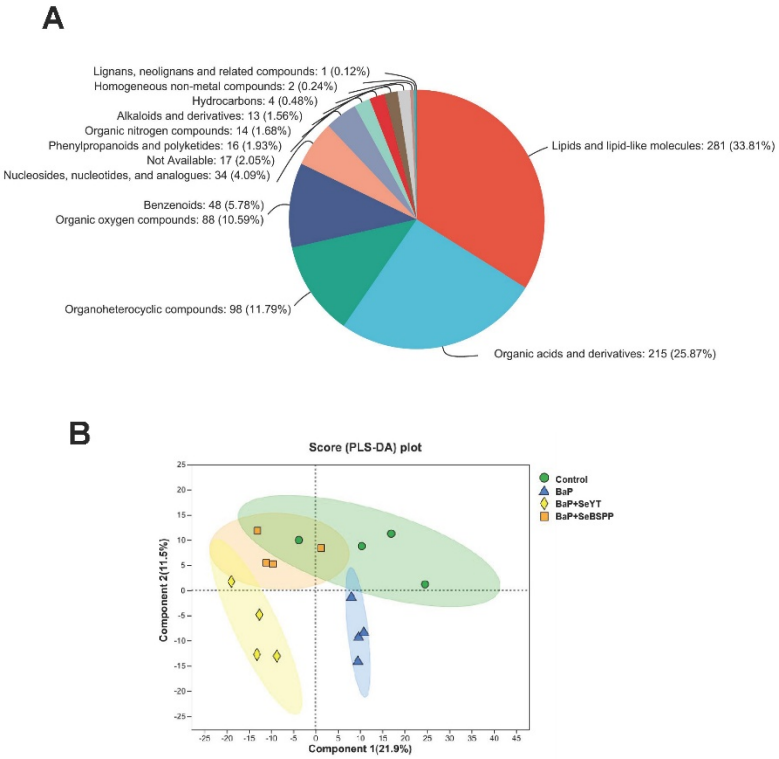

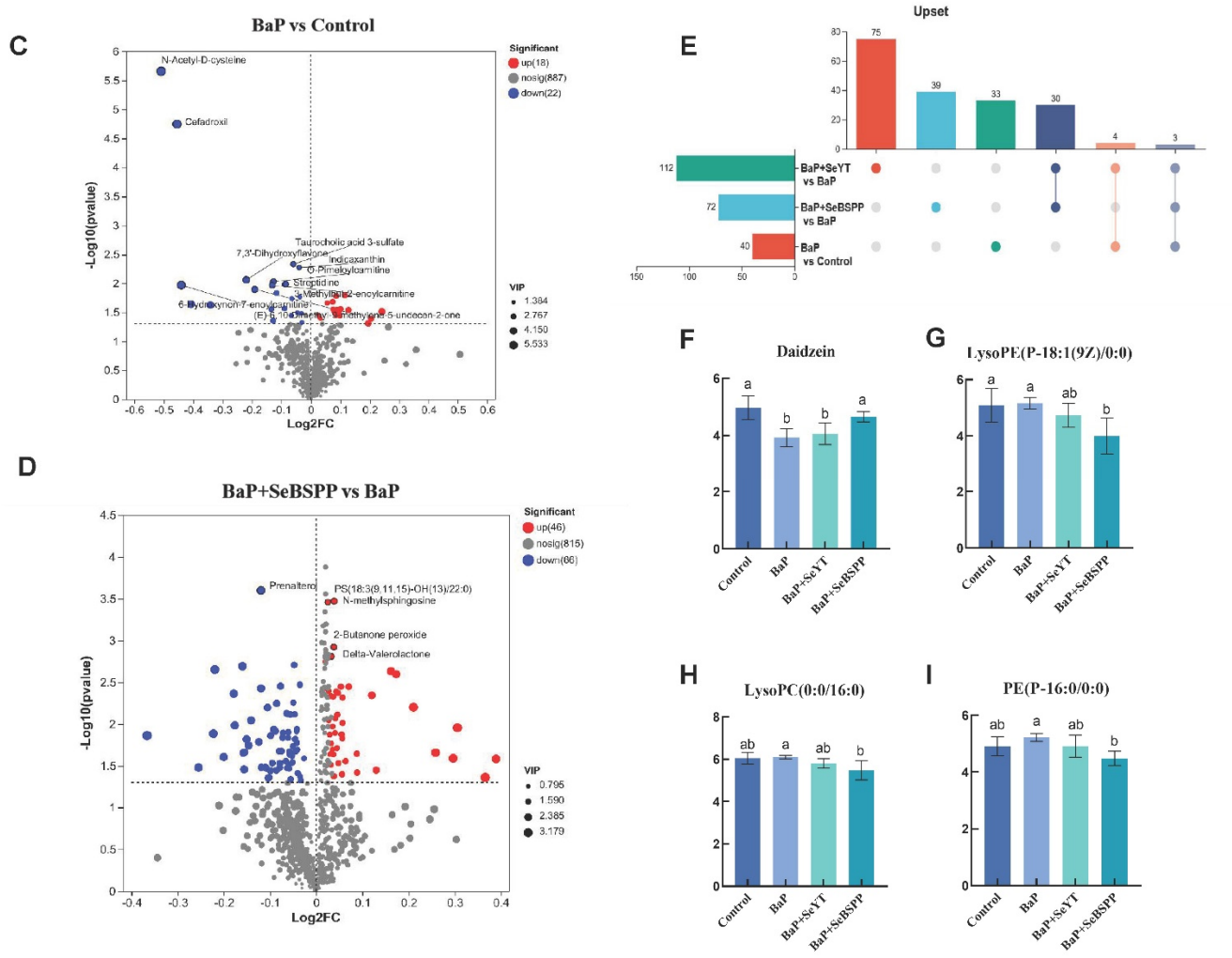

Figure 3. SeBSPP impact on liver metabolites.
(A) Metabolite composition; (B) PLS-DA anlysis of Control, BaP, BaP+SeBSPP and BaP+SeYT; (C) Volcano plot of differential metabolites in BaP vs Control; (D) Volcano plot of differential metabolites in BaP+SeBSPP vs BaP; (E) Upset of differentially expressed metabolites among four groups; (F) The abundance of Daidzein; (G) The abundance of LysoPE(P-18:1(9Z)/0:0); (H) The abundance of LysoPC(0:0/16:0); (I) The abundance of PE(P-16:0/0:0). These results are shown as the means ± SD, with 6 mice/group, $P < 0.05$. PLS-DA: Partial least squares discrimination analysis.

3.5 Effects of SeBSPP on gut microbiota

Gut microbiota are important regulators of health, and disruptions in the gut microbial communities emerges the leading cause of liver dysfunctions. Hepatic steatosis and hepatotoxicity were closely related to dysbiosis of gut microbiota[0]. We thus evaluated impacts of SeBSPP on the gut microbiome of Bap-treated mice and compared its efficacy with SeYT. BaP had no impact on α-diversity of gut microbiota compared with the Control group (Fig. 4A-D). Compared with BaP, SeBSPP and SeYT increased α-diversity and number of detected bacteria, substantially altering gut microbiota compositions (Fig. 4E). SeBSPP exhibited a notable presence of unique bacteria (Supple. 1C).

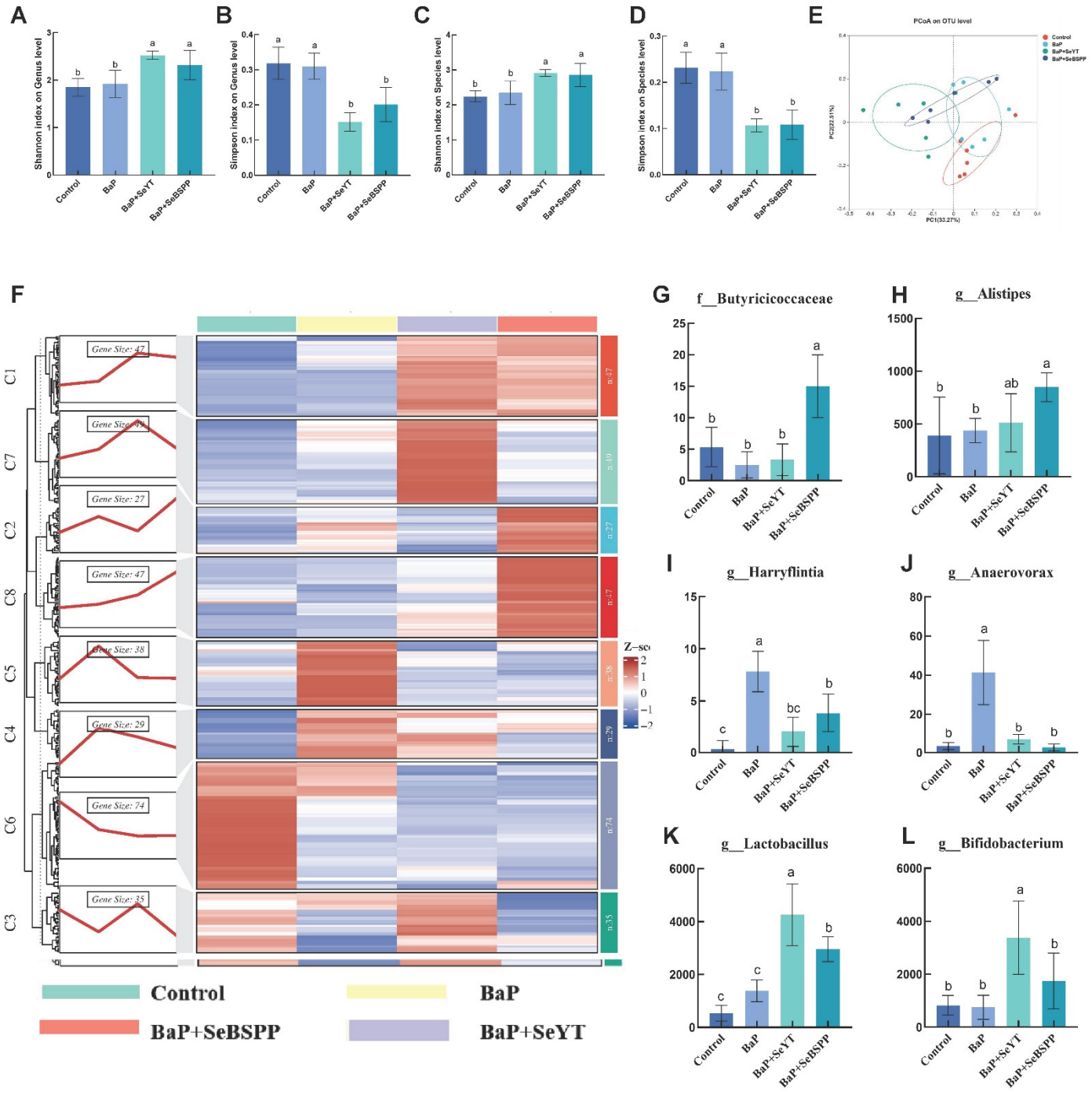

Figure 4. SeBSPP impact on gut microbiota composition.

(A) Shannon index on Genus level of Control, BaP, BaP+SeBSPP and BaP+SeYT; (B) Simpson index on Genus level of Control, BaP, BaP+SeBSPP and BaP+SeYT; (C) Shannon index on Species level of Control, BaP, BaP+SeBSPP and BaP+SeYT; (D) Simpson index on Species level of Control, BaP, BaP+SeBSPP and BaP+SeYT; (E) PCoA anlysis of Control, BaP, BaP+SeBSPP and BaP+SeYT; (F) Cluster analysis of expression trends on the family, genus and specifications levels of gut microbiota; (G) The relative abundance of *f__Butyricicoccaceae*; (H) The relative abundance of *g__Alistipes*; (I) The relative abundance of *g__Harryflintia*; (J) The relative abundance of *g__Anaerovorax*; (K) The relative abundance of *g__Lactobacillus*; (L) The relative abundance of *g__Bifidobacterium*. These results are shown as the means ± SD, with 6 mice/group, $P < 0.05$.

Trend clustering revealed distinct patterns of bacteria taxa responses to the different treatments (Fig. 4F). A total of 8 clusters was determined. Specifically, BaP increased relative abundances of gut microbiota that were clustered in the C4 (n=28) and C5 (n=37), including *g.__Anaerovorax, g__Butyricicoccus, g__Eubacterium_xylanophilum_group* and *g.__Harryflintia*, compared with Control. In contrast, BaP

lowered abundances of bacteria clustered in the C3 (n=34), such as *g__Alloprevotella, g__Akkermansia, g__Rikenellaceae_RC9_gut_group* and *g__Streptococcus*. SeBSPP and SeYT could restored BaP-induced abnormalities in gut microbiota. Specifically, SeBSPP pre-feeding significantly reduced *g.__Anaerovorax* and *g.__Harryflintia.*, leading to abundances resembling Control (Fig. 4I&J). Moreover, SeBSPP uniquely induced increases in *g.__Alistipes*, *f.__Butyricicoccaceae.g_UCG.009* and *g.__Lactobacillus* (Fig. 4G, H&K). Besides, *g.__Lactobacillus* and *g.__Bifidobacterium* were highest in SeYT than others (Fig. 4K&L). These data reflected that SeBSPP and SeYT pre-feeding altered the diversity and composition of gut flora.

Short-chain fatty acids (SCFAs) are the product of carbohydrate or amino acid breakdown by gut flora and can reduce hepatic lipid accumulation, by activating PPARγ[0]. We examined the levels of some short chain fatty acids. Significantly, BaP decreased the levels of SCFAs in the colon compared with control. While SeBSPP and SeYT pretreatment effectively increased SCFAs levels (Fig. 5A-D). We also validated PPARγ protein levels by western blot (Fig. 5E).

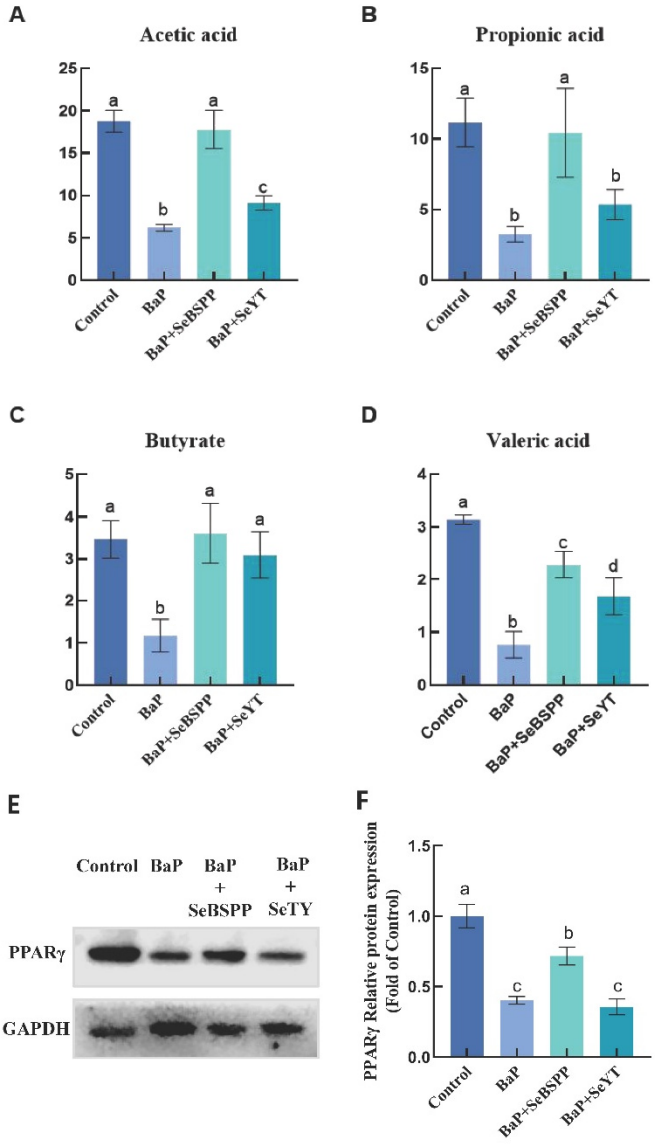

Figure 5. SeBSPP impact on SCAFs and PPARγ levels.
(A) Acetic acid; (B) Propionic acid; (C) Butyrate; (D) Valeric acid; (E) Western Blot of PPARγ; (F) PPARγ Relative protein expression (Fold of Control). These results are shown as the means ± SD, with 6 mice/group, $P < 0.05$. SCAFs: Short-chain fatty acid.

3.6 Integration of SeBSPP-modulated genes, metabolites and gut microbiota

A total of 78 intestinal flora in C1, C2, C3, C5, C7 and C8 groups under genus classification was selected for further fusion analysis WGCNA modelling was adopted to identify highly synergistic expressed modules containing core genes (n=222), metabolites (n=112) and gut microbes (n=78) that were predominately modulated by SeBSPP, resulting in the 3 expression modules (Fig. 6A). WGCNA-derived modules, in particular, grey(n=91), strongly correlated with biochemical parameters of liver functions (Fig. 6B), including H_2O_2, MDA, TC, TG, AST, ALT, AhR, *Cyp1a1*, SOD and GSH ($P < 0.05$). Furthermore, blue(n=111), strongly correlated with TC, TG, ALT, H_2O_2, SOD and GSH ($P < 0.05$).

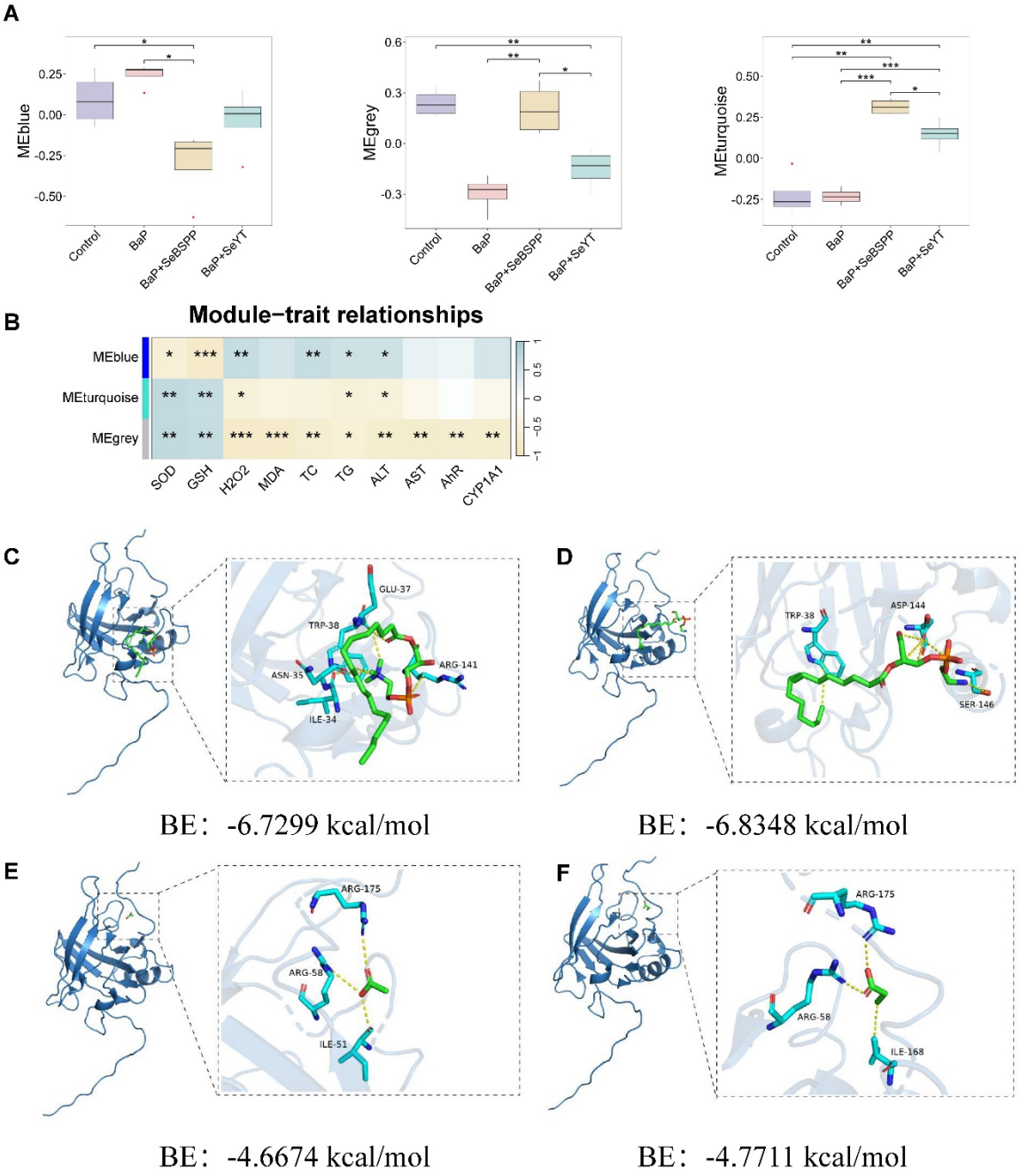

Figure 6. Comprehensive analysis of the impact of SeBSPP by WGCNA.
(A) WGCNA module; (B) Correlation heatmap of biological indicators and WGCNA modules; (C) Acetic acid-Mup11 molecular docking; (D) Butyrate-Mup11 molecular docking; (E) LysoPC(17:0/0:0)-Mup11 molecular docking; (F) LysoPE(0:0/16:0)-Mup11 molecular docking. WGCNA: Weighted gene coexpression network analysis.

Hub gene *Mup11,* lipid metabolites including LysoPC(17:0/0:0) and LysoPE(0:0/16:0) and short-chain fatty acid aceticacid and butyrate were selected for molecular docking by MOE 2019 software (Fig. 6C-F). According to the binding results, the molecular docking energy range is -4.1727~-6.8348 kcal/mol. It is generally believed that the docking energy value of < -4.25 kcal/mol indicates binding activity between the two, < -5.0 kcal/mol indicates good binding activity, < -7.0 kcal/mol indicates strong binding activity, and the lower the binding energy, it means that the small molecule active ingredient may have stronger binding activity with the target. The docking results showed that LysoPC(17:0/0:0)-*Mup11* (BE: -6.7299 kcal/mol） and LysoPE(0:0/16:0)-*Mup11* (BE:-6.8348 kcal/mol) had good binding activity, aceticacid-*Mup11* (BE: -4.6674 kcal/mol) and butyrate-*Mup11* (BE: -4.1727 kcal/mol) had binding activity.

4. Discussion

Numerous studies have demonstrated the hepatotoxic effects of BaP. For instance, BaP exerts significant damage on liver cells by inducing both autophagy and pyroptosis, processes that mutually reinforce each other, as confirmed in our previous research[0]. Additionally, BaP can trigger oxidative stress and inflammation in the livers of mice[0]. Prior investigations have also shown that Se-rich products, such as Se-rich rice[0], exhibit certain hepatoprotective properties. In this study, we found that SeBSPP alleviated BaP-induced liver damage by regulating *Cyps*, lipid metabolism, and intestinal flora imbalance.

When BaP enters the body, it activates AhR, triggering its translocation from the cytoplasm to the nucleus and upregulating the expression of *Cyp1a1* and *Cyp1b1*. BaP is then metabolized by CYP450 enzymes into toxic metabolites, among which BPDE exhibits the strongest mutagenic potential, forming bulky DNA adducts known as BPDE-DNA[0,0]. Our study found that SeBSPP significantly suppresses the toxicity of BaP. SeBSPP exerts its protective effects by modulating multiple pathways, including steroid hormone biosynthesis and chemical carcinogenesis-DNA adducts formation, primarily through the downregulating *Cyps* such as *Cyp1a1*, *Cyp2c40*, *Cyp2c39*, and *Cyp3a44.* These genes are not only involved in linoleic acid metabolism, retinol metabolism, steroid hormone biosynthesis, and arachidonic acid metabolism, but also play roles in the regulation of inflammatory mediator signaling via TRP channels and in chemical carcinogenesis through DNA adduct formation.

SeBSPP effectively alleviated liver dusfunction and hepatic oxidative damage. As the primary target organ of BaP, the liver has been shown to exhibit significantly elevated levels of TC, TG, AST, and ALT in mice exposed to BaP[0]. Consistent with previous studies, the BaP treatment group displayed markedly higher levels of these markers in serum compared to the Control group. However, prior administration of SeBSPP and SeYT resulted in a noticeable decrease in these makers compared to the group treated with BaP alone. Moreover, the activities of MDA, H_2O_2, GSH-Px, and SOD commonly used antioxidant indicators, clearly demonstrated the antioxidant capacity of SeBSPP[00]. Additionally, we observed a significant increase in daidzein levels in the SeBSPP pre-treatment group, which is predominantly found in leguminous plants, is known for its strong antioxidant properties[0].

Liver is the primary organ responsible for the synthesis and metabolism of endogenous metabolite such as lysophosphatidylcholine (LPC) and amino acids. Liver damage inevitably leads to alterations in the levels and metabolic processes of LPC and amino acids in the body[0]. Studies have shown that both obese and diabetic individuals exhibit elevated levels of branched-chain amino acids (BCAAs), including leucine, isoleucine, and valine, while levels of glutamine and glycine levels are reduced[00]. SeBSPP was found to uniquely upregulate the glutamine-glutamate, while simultaneously downregulating leucine, isoleucine, and valine. Moreover, SeBSPP effectively inhibited fatty acid elongation by downregulating the expression of *Acot1*, *Elovl5, Elovl3*, resulting in reducing levels of long-chain saturated fatty acid. These findings indicate that SeBSPP play a beneficial role in improving hepatic lipid metabolism.

There is a unique anatomical and functional relationship between the intestine and the liver. The composition and abundance of the intestinal microbiota can influence liver health. Disruption of the intestinal microbiota can damage the intestinal mucosal barrier, allowing bacteria and toxins enter the liver, thereby exacerbating liver inflammation and lipid accumulation, conversely, the supplementation of probiotics has been shown to reduce liver injury and improve liver function[00]. Behrouz et al. found that *g. _Bifidobacterium* may help improve liver enzymes and lipid profiles in patients with non-alcoholic fatty liver disease (NAFLD)[0]. Ji et al. also reported that g._Lactobacillus can regulate liver lipid metabolism by downregulating key enzymes such as acetyl-CoA carboxylase, fatty acid synthase, and stearoyl-CoA desaturase-1 in the liver[0]. Furthermore, *g._Akkermansia* has been most strongly linked to hypertriglyceridemia, hyperglycemia, and reduced HDL cholesterol[0]. SeBSPP can counteract the effect of BaP on the gut microbiota and increase the abundance of intestinal flora.

Meanwhile, SCFAs, as metabolites of gut microbiota, play a crucial role in the gut-liver axis. Acetic acid has been shown to effectively inhibit lipid synthesis in the liver and reduce serum levels of TC and TG in mice[0]. SCFAs can also activate PPARγ, a key regulator involved in adipocyte differentiation and glucose homeostasis[0]. Furthermore, we found that butyrate and acetic acid are capable of regulating *Mup11* expression. *Mups* are involved in various functions, including lipid metabolism, carbohydrate metabolism, and signal recognition. *Mups* are closely associated with glucose and lipid metabolism. They can attenuate the ability of cAMP analog (glucagon mimetic) and dexamethasone (glucocorticoid mimetic) to stimulate hepatic glucose production, and suppress the expression of both gluconeogenic and lipogenic genes in the liver[0]. Additionally, *Mup11* belongs to the lipocalin family and is responsible for transporting small hydrophobic molecules, such as lipids and volatile pheromones[0]. Our findings indicate that *Mup11* can inhibit the levels of long-chain saturated fatty acids, such as LPE(0:0/16:0) and LPC((17:0/0:0). These long-chain saturated fatty acids are involved in liver lipid metabolism[00] and have been found to be positively associated with non-alcoholic fatty liver disease[0]. The increased expression of *Mup11* and *Mup1* in the SeBSPP+BaP group suggests a significant alteration in intracellular lipid transport in mice. Overall, SeBSPP effectively mitigates liver lipid metabolic injury by modulating the gut-liver axis.

5. Conclusion

In conclusion, SeBSPP could attenuated BaP induced liver injury through reducing liver oxidative damage, inhibiting BaP metabolism, improving liver lipid metabolism, and regulating the intestinal microbiota (Fig. 7). Our study provides a reference for investigating the beneficial effects of Se-enriched plant polypeptide and for the development of Se-enriched food supplement. In future research, we aim to further explore the potential interaction between AhR and short chain fatty acids.

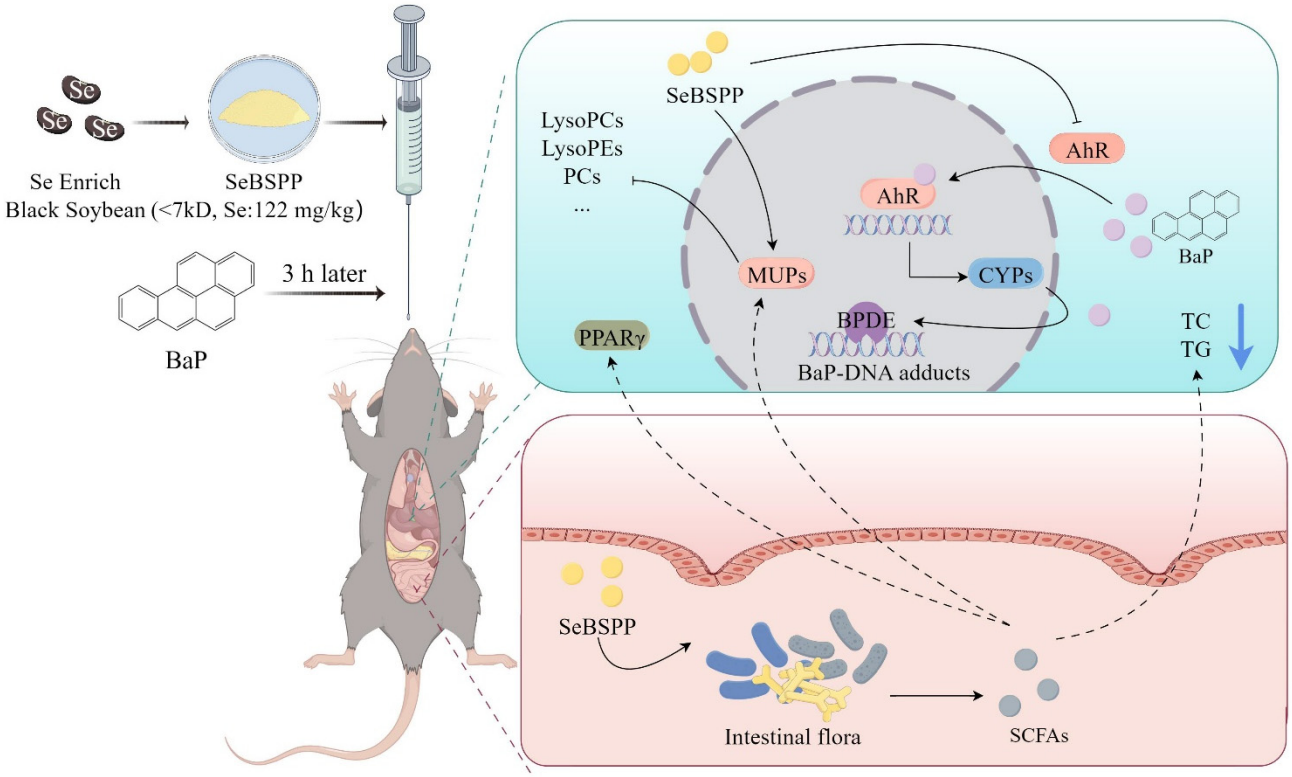

Figure 7. Overall summary of the effects of SeBSPP on liver injury and gut dysbacteria induced by BaP. (By Figdraw)

Declarations of Competing interest

The authors declare no conflicts of interest and disclose non-financial interests.

Acknowledgments

This work was financially supported by the National Natural Science Foundation of China (31972183), the Regional Innovation Capability Guidance Program of Shaanxi Province (2022QFY09-03) and the Training Program of Excellent Youth Innovation Team (GK202401006).

Data availability

The data underlying this article are available in the article and in its online supplementary material.

Reference

J. Ge, R. Hao, X. Rong, et al. Secoisolariciresinol diglucoside mediated p38 and ERK pathway. Food Chem Toxicol, 2022. 159: 112733. https://doi:10.1016/j.fct.2021.112733

M. L. Salem, N. E. El-Ashmawy, E. E. Abd El-Fattah, et al. Immunosuppressive role of Benzo[a]pyrene in induction of lung cancer in mice. Chem Bio Interact, 2021. 333: 109330. https://doi:10.1016/j.cbi.2020. 109330

X. Ji, Y. Li, J. He, et al. Depletion of mitochondrial Enzyme system in liver, lung, brain, stomach and kidney induced by benzo(a)pyrene. Environ Toxicol Phar, 2016. 43: 83-93. https://doi:10.1016/ j.etap.2016. 03.001

B. Bukowska, P. Sicińska. Influence of Benzo(a)pyrene on Different Epigenetic Processes. Int Journal Mol Sci, 2021. 22(24): 13453. https://doi:10.3390 /ijms222413453

J. Q. Ma, C. M. Liu, Z. H. Qin, et al. Ganoderma applanatum terpenes protect mouse liver against benzo(a)pyren-induced oxidative stress and inflammation. Environ Toxicol Phar, 2011. 31: 460-468. https://doi:10. 1016/j.etap.2011.02.007

Y. Jiang, X. Zhou, X. Chen, et al. Benzo(a)pyrene-induced mitochondrial dysfunction and cell death in p53-null Hep3B cells. Mutat. Res., Genet Toxicol Environ Mutagen. 2011. 726: 75-83. https://doi:10.1016/j.mrgentox.2011.08.006

C. Z. Chung, N. Krahn. The selenocysteine toolbox: A guide to studying the 21st amino acid. Arch Biochem Biophys, 2022. 109421. https://doi: 10.1016 /j.abb.2022.109421

A. Ostrozka-Cieslik, B. Dolinska, F. Ryszka. Therapeutic potential of selenium as a component of preservation solutions for kidney transplantation. Molecules, 2020. 25(16): 3592. https://doi: 10.3390/molecules25163592

A. C. Ruberte, C. Sanmartin, C. Aydillo, et al. Development and therapeutic potential of selenazo compounds. J Med Chem, 2020. 63(4): 1473-1489. https://doi:10.1021/acs.jmedchem. 9b01152

D. N. Nguyen, P. V. Dang, Q. A. Le, et al. Preparation and effect of selenium nanoparticles/oligochitosan on the white blood cell recovery of mice exposed to gamma-ray radiation. J Chem, 2021. 2021: 6635022. https://doi. org/10.1155/2021/6635022

T. Yu, J. Guo, S. Zhu, et al. Protective effects of selenium-enriched peptides from Cardamine violifolia against high-fat diet induced obesity and its associated metabolic disorders in mice. RSC Advances, 2020. 10(52):31411-31424. https://doi.org/10.1039/ D0RA04209A

J. Zhang, W. Li, H. Li, et al. Selenium-Enriched Soybean Peptides as Novel Organic Selenium Compound Supplements: Inhibition of Occupational Air Pollution Exposure-Induced Apoptosis in Lung Epithelial Cells. Nutrients, 2023. 16(1):71. https:// doi:10.3390/nu16010071

Z. Wang, L. Shi, H. Li, W. Song, J. Li, L.Yuan. Selenium-Enriched Black Soybean Protein Prevents Benzo(a)pyrene-Induced Pyroptotic Colon Damage and Gut Dysbacteriosis. J Agric Food Chem, 2022.70(39):12629-12640. https://doi: 10.1021/acs.jafc.2c04526

K. R. LeFort, W. Rungratanawanich, B. J. Song. Contributing roles of mitochondrial dysfunction and hepatocyte apoptosis in liver diseases through oxidative stress, post-translational modifications, inflammation, and intestinal barrier dysfunction. Cell Mol Life Sci, 2024. 81(1):34. https://doi:10. 1007/s00018-023-05061-7

K. C. Bauer, P. T. Littlejohn, V. Ayala. Nonalcoholic fatty liver disease and the gut-liver axis: Exploring an undernutrition perspective. Gastroenterology, 2022. 162(7): 1858-1875. https://doi: 10.1053/j.gastro.2022.01.058

J. Rong, Z. Zhang, X. Peng, et al. Mechanisms of hepatic and renal injury in lipid metabolism disorders in metabolic syndrome. Int J Biol Sci, 2024. 20(12):4783-4798.https://doi: 10. 7150/ijbs.100394

S. He, X. Li, C. Li, et al. Isoorientin attenuates benzo[a]pyrene-induced colonic injury and gut microbiota disorders in mice. Food Res Int, 2019. 126:108599. https://doi.org/10.1016/j.foodres.2019.1085 99

Y. Li. Su, F. Ling, U. H. Muhammad, et al. Rescue effects of Se-enriched rice on physiological and biochemical characteristics in cadmium poisoning mice. Environ Sci Pollut Res, 2021. 28: 20023-20033.https://doi:10.1007 /s11356-020-11854-1

Y. Tanaka, T. Ito, G. Tsuji, et al. Baicalein inhibits benzo[a]pyrene-induced toxic response by downregulating Src phosphorylation and by upregulating NRF2-HMOX1 system. Antioxidants (Basel), 2020. 9(6): 507. https://doi: 10.3390/antiox9060507

C. J. MacDonald, R. Y. S. Cheng, D. D. Roberts, et al. Modulation of carcinogen metabolism by nitric oxide-aspirin 2 is associated with suppression of DNA damage and DNA adduct formation. J Biol Chem, 2009. 284(33): 22099-22107. https://doi:10.1074/jbc.M109.021063

M. A. Alzohairy, A. A. Khan, M. A. Alsahli, et al. Protective effects of thymoquinone, an active compound of nigella sativa, on rats with benzo(a)pyrene-induced lung injury through regulation of oxidative stress and inflammation. Molecules, 2021. 26(11): 3218. https://doi:10.3390/ molecules26113218

J. Dworzański, M. Strycharz-Dudziak, E. Kliszczewska, et al. Glutathione peroxidase (GPx) and superoxide dismutase (SOD) activity in patients with diabetes mellitus type 2 infected with Epstein-Barr virus. PLoS One, 2020. 15(3): 0230374. https://doi:10. 1371/journal.pone.0230374.

M. M. Alshehri, J. Sharifi-Rad, J. Herrera-Bravo, et al. Therapeutic potential of isoflavones with an emphasis on daidzein. Oxid Med Cell Longevity, 2021. 6331630. https://doi:10.1155/ 2021/6331630

C. Hu, H. W. Li, J. Q. Ke, et al. Metabolic profiling of lysophosphatidylcholines in chlorpromazine hydrochloride- and N-acetyl-p-amino-phenoltriptolide-induced liver injured rats based on ultra-performance liquid chromatography quadrupole time-of-flight mass spectrometry. Hum Exp Toxicol, 2022. 41: 9603271221108320.https://doi:10.1177/0960 3271221108320

C. Hu, H. Li, L. Wu, et al. Metabolic profiling of 19 amino acids in triptolide-induced liver injured rats by gas chromatography-triple quadrupole mass spectrometry. Hum Exp Toxicol, 2021. 40:1685-1697.https://doi:10.1177/ 09603271211006167

C. B. Newgard, J. An, J. R. Bain, et al. A branched-chain amino acid-related metabolic signature that differentiates obese and lean humans and contributes to insulin resistance. Cell Metabolism, 2009. 9:311-326. https://doi:10. 1016/ j. cmet.2009.02.002

J. Fang, C. H. Yu, X. J. Li, et al. Gut dysbiosis in nonalcoholic fatty liver disease: pathogenesis, diagnosis, and therapeutic implications. Front Cell Infect Microbiol, 2022. 12:997018. https://doi: 10.3389/fcimb.2022.997018

E. Rebelos, P. Iozzo, M. A. Guzzardi, et al. Brain-gut-liver interactions across the spectrum of insulin resistance in metabolic fatty liver disease. World J Gastroenterol, 2021. 27(30): 4999-5018.https://doi: 10.3748/wjg.v27.i30.4999

V. Behrouz, N. Aryaeian, M. J. Zahedi, et al. Effects of probiotic and prebiotic supplementation on metabolic parameters, liver aminotransferases, and systemic inflammation in nonalcoholic fatty liver disease: A randomized clinical trial. J Food Sci, 2020. 85:3611-3617. https://doi: 10.1111/1750-3841.15367

Y. S. Ji, H. N. Kim, H. J. Park, et al. Modulation of the murine microbiome with a concomitant anti-obesity effect by Lactobacillus rhamnosus GGand Lactobacillus sakei NR28. Beneficial Microbes, 2012. 3:13-22. https://doi:10.3920/ BM2011.0046

Q. Zhou, G. Pang, Z. Zhang, et al. Association between gut akkermansia and metabolic syndrome is dose-dependent and affected by microbial interactions: a cross-sectional study. Diabetes, Metab Syndr Obes.: Targets Ther, 2021. 14:2177-2188. https://doi:10.2147/DMSO.S311388

J. Liu, W. Bao, M. Jiang, et al. Chromium, selenium, and zinc multimineral enriched yeast supplementation ameliorates diabetes symptom in streptozocin-induced mice. Biol Trace Elem Res, 2012.146(2):236-245. https://doi: 10.1007/s12011-011-9248-x

Y. Zhou, L. Jiang, L. Rui. Identification of MUP1 as a regulator for glucose and lipid metabolism in mice. J Biol Chem, 2009. 284(17):11152-11159. https://doi: 10.1074/jbc. M900754200

R. S. Dewal, F. T. Yang, L. A. Baer, et al. Transplantation of committed pre-adipocytes from brown adipose tissue improves whole-body glucose homeostasis. iScience, 2024. 27:108927.https://doi:10.1016/j.isci.2024.108927

Z. Li, L. B. Agellon, T. M. Allen, et al. The ratio of phosphatidylcholine to phosphatidylethanolamine influences membrane integrity and steatohepatitis. Cell Metabolism, 2006. 3(5):321-331. https://doi: 10.1016/j.cmet. 2006.03.007

D. Djekic, R. Pinto, D. Repsilber, et al. Serum untargeted lipidomic profiling reveals dysfunction of phospholipid metabolism in subclinical coronary artery disease. Vasc Health Risk Manage, 2019. 15:123-135. https://doi:10.2147/ VHRM.S202344

Y. Deng, M. Pan, H. Nie, et al. Lipidomic analysis of the protective effects of Shenling Baizhu San on non-alcoholic fatty liver disease in rats. Molecules, 2019. 24(21):3943-3960. https://doi:10.3390/molecules24213943